Ann. Rev. Fluid Mech. 1988. 20: 325–57

FOAM FLOWS[1]

Andrew M. Kraynik

Fluid and Thermal Sciences Department, Sandia National Laboratories, Albuquerque, New Mexico 87185

INTRODUCTION

A foam is a structured fluid in which gas bubbles are separated by thin liquid films and the volume fraction of the continuous liquid phase is small. While polyhedral air bubbles dispersed in a network of soap films provide a familiar prototype, concentrated liquid-liquid emulsions display many of the same characteristics. The liquid phase in persistent foams always contains a surface-active agent that preferentially accumulates at the gas-liquid interfaces and imparts varying degrees of stability to the films. The surfactancy, thin films, and large interfacial area associated with metastable foams place them in the domain of colloid and interface science. Interfacial phenomena are central to cell-level mechanisms that determine the complex rheological behavior of foams—behavior that one could not anticipate by knowing the physical properties of the constituent phases alone.

Typical cell dimensions (10 μm–1 cm), which serve as a natural length scale ℓ for the foam structure, are much larger than the very fine scale dimensions of simple molecules that compose Newtonian fluids. The large magnitude of ℓ promotes strong interactions between the foam structure and the flow, and these give rise to non-Newtonian rheological effects. The engineer requires a description of foam flow that applies over macroscopic length scales that are much larger than ℓ. Two flow regimes can be distinguished by comparing ℓ with $\mathscr{L}$, where $\mathscr{L}$ is a characteristic length scale for the space that confines the flow. Foam flow through pipes is a typical *macroflow*, which is characterized by $\ell \ll \mathscr{L}$. While a continuum description may apply to the macroflow, the constitutive relation for the

[1]The US Government has the right to retain a nonexclusive royalty-free license in and to any copyright covering this paper.

bulk foam will be nonlinear and the usual no-slip boundary condition may not be valid at solid surfaces. The formidable rheological complexity of macroflows carries over to *microflows*, where $\ell \approx \mathscr{L}$. Foam flow in a porous medium exemplifies the microflow regime, in which continuum concepts such as foam viscosity are invalid because the dimensions of bubbles and the minute pore spaces are comparable. Darcy's law and conventional two-phase flow theory represent few features of foam displacement in porous media. The structure of foam clearly depends upon the ratio $\ell/\mathscr{L}$. In macroflows, bulk foams are relatively unconstrained when compared with microflows in fine capillary tubes and porous media, where elongated bubbles conform to solid boundaries and occur individually or in trains.

The systematic study of foam flow draws upon numerous scientific disciplines, with surface science foremost. Because liquid films control foam structure, physicochemical principles established from studies of isolated soap films are fundamental to foam rheology. Molecular and macroscopic mechanisms that determine the stability of films, their mechanical response, and their conformation have been described by Mysels et al. (1959), Bikerman (1973), Rosen (1978), and Lucassen (1981). Slattery & Flumerfelt (1982) have discussed balance laws and constitutive equations that relate to the interfacial region. The presence of surfactants and their transport influence fluid microstructure and fluid mechanics at the film level. The fundamental difficulties and uncertainties connected with the interfacial and intralamellar regions carry over to the description of foam flow.

This review should be more appropriately considered a preview of issues relating to foam flow, many of which are unresolved or unaddressed. The flow of bulk foams (the macroflow regime) is emphasized. Experimentalists and theorists will find foam flows challenging because these multiphase fluids are compressible, nonlinear, viscoelastic materials with striking metastability characteristics. Like solids, foams possess a finite shear modulus. But unlike them, foams flow and their flow behavior is characterized by a yield stress, shear-thinning viscosity, and slip at the wall. Many of these phenomena have counterparts in porous media, where the cell-level mechanisms are different. Such microflows are beyond the scope of this article. Adler & Brenner (1988) review multiphase flow in porous media elsewhere in this volume.

PRACTICAL MOTIVATIONS

Applications involving the flow of foam have not been completely inhibited by unresolved fundamental issues. The usefulness of aqueous foams in fire

fighting motivated early studies of pipe flow; however, technology in the oil and gas industry has provided the greatest incentive to developing an understanding of foam flow in pipes as well as porous media. The highly viscous nature of foams benefits the transport of particulates in well drilling and clean-out operations. In foam fracturing, proppant particles (typically sand) are carried into hydraulic fractures in geological formations to prevent the fractures from closing. Evidence that foam mobility in porous media decreases as formation permeability increases suggests that foams may be useful as blocking and diverting agents, which permit a degree of control over the path of reservoir fluids. In principle, foam offers a spectrum of mobility characteristics in porous media and shows promise for use in a wide range of mobility control applications relating to enhanced oil recovery. The reviews of Heller & Kuntamukkula (1987) and Assar & Burley (1986) cover the petroleum literature on foam flow.

Foam is also a candidate for transporting pulverized coal in pipelines. In addition, it is an attractive vehicle for dispersing pigments and other surface treatments in paper coating and fabric finishing, where the energy budget for drying is important. Liquid foam is often an intermediate stage in processing synthetic cellular solids, such as rigid and flexible polymeric "foams." Since structure influences the properties of these materials, there is incentive to understand the role of flow in the development of cell morphology and the orientation of macromolecules and microphases. It is also desirable to be able to substitute predictive models for empiricism, like that proposed to correlate certain features of thermoplastic foam extrusion where the dispersed phase nucleates and expands during flow through a die (Kraynik 1981).

FOAM STRUCTURE

The structure of bulk foam is basic to understanding its rheology but difficult to quantify, even though elementary features are obvious. By observing multiple soap bubbles and soap films supported on wire frames, Plateau (1873) recognized that three films, each with its own uniform total curvature, always meet at equal dihedral angles of 120°. The film junction regions, now called *Plateau borders*, determine the edges of polyhedral gas bubbles. Four such edges always join at equal angles of $\cos^{-1}(-1/3) \approx 109.47°$. Planar films cannot satisfy the latter constraint because a planar polygon cannot have all angles equal to 109.47°; this necessitates curved films with complicated shapes. These structural characteristics balance film tension and minimize surface energy.

Kelvin (1887), in pursuit of ideal foam structure, showed that space

could be partitioned into identical cells of equal volume and minimal surface area. His isotropic, minimal tetrakaidecahedron (a modified truncated octahedron) contains six planar quadrilateral and eight nonplanar hexagonal faces, all with curved edges. It is striking that Matzke (1946) did not find a single fourteen-sided cell with this edge and face distribution during meticulous observations of 600 bubbles in "monodisperse" foams. In fact, pentagonal faces were predominant, and they are not even represented in Kelvin's tetrakaidecahedron. Matzke's extensive statistics indicates that a type cell does not exist; nevertheless, idealized foam cells that are based upon various plane-faced polyhedra are useful for relating phase volume fractions to structural parameters, such as cell size, film thickness, and Plateau border curvature (Princen et al. 1980). Some model cells, like that based upon the regular pentagonal dodecahedron, do not fill space; none satisfy equilibrium requirements.

The complexity of three-dimensional structure perhaps explains why progress in developing micromechanical theories for foam rheology has been restricted to two-dimensional models, which preserve some essential features of the Plateau borders. While the spatial arrangement of films is important, one cannot overemphasize the significance of Plateau borders in foam transport phenomena.

DILUTE EMULSIONS AND GAS-BUBBLE SUSPENSIONS

Before describing models of foam rheology, it is instructive to review theories that apply to dilute gas-bubble suspensions, the other extreme in volume fraction. This permits one to compare and contrast the rheology and physical mechanisms for the two concentration regimes. In typical polymeric foam fabrication processes, the dispersion passes through various volume-fraction and rheological regimes as a single-phase fluid develops into a cellular material, so the dilute regime is of practical interest. Unlike foams, their dilute counterparts have accounted for substantial activity within the traditional suspension rheology community. In part, the progress is due to an emphasis on single "particles" and the mathematical techniques available for solving the Stokes equations.

Taylor (1932) has shown that when shear rates are small enough for drop deformation to be neglected, the effective viscosity μ_e of a dilute emulsion of neutrally buoyant drops is given by

$$\mu_e = \mu\left\{1+\phi_d\left[\frac{5\lambda+2}{2(\lambda+1)}\right]\right\}, \tag{1}$$

where μ is the continuous-phase viscosity, λ is the viscosity ratio μ^*/μ (μ^* refers to the viscosity of the dispersed phase), and ϕ_d is the volume fraction of the dispersed phase (which is assumed small). Einstein's result for a suspension of rigid spheres is recovered when $\lambda \to \infty$. The effective viscosity for a dilute suspension of spherical gas bubbles, for which $\lambda \to 0$, is $\mu_e = \mu(1+\phi_d)$. Since the presence of the bubble disturbs the external flow, the effective viscosity exceeds that of the continuous phase, even when the bubble is inviscid. Passing to the limit $\lambda \to 0$ is within the scope of Taylor's analysis; however, replacing a neutrally buoyant drop with a much lighter gas bubble is not, when gravity acts. Velocity disturbances for sedimentation can be neglected relative to those for macroscopic shearing flow when $a\rho' g/\mu\dot{\gamma} \ll 1$, where a is the droplet radius, ρ' the density difference, g the acceleration due to gravity, and $\dot{\gamma}$ the macroscopic deformation rate. This foretells the difficulty of defining a rest state for foam.

Schowalter et al. (1968) extended Taylor's theory to account for drop deformation in steady homogeneous shearing flow. When λ is not too large, small departures of drop shape from sphericity depend upon a capillary number $\mathrm{Ca} = \mu a\dot{\gamma}/\sigma$, where σ is the interfacial tension. The capillary number is a relative measure of viscous forces that tend to distort the drop and interfacial tension, which favors sphericity. Drop distortion manifests itself as non-Newtonian behavior with finite normal-stress differences. The primary and secondary normal-stress functions of viscometric flow (Schowalter 1978), for $\lambda \to 0$, are $N_1 = 32\phi_d\mu^2 a\dot{\gamma}^2/5\sigma$ and $N_2 = -25N_1/56$, where $\dot{\gamma}$ now represents the shear rate. The signs and relative magnitudes of these functions are in accord with those for polymer melts and solutions.

While Schowalter et al. obtained viscometric functions, they could only infer the proper form of the constitutive equation for dilute emulsions from their steady-state analysis. Building upon the perturbation analysis of Cox (1969) for the response of a drop to time-varying shear flow, Frankel & Acrivos (1970) derived a nonlinear constitutive equation for dilute emulsions that accounts for unsteady flow. Schowalter (1978) has provided an insightful account of these developments.

The previous analyses assume the simplest interfacial boundary condition—that tangential stress components are continuous across the drop interface and normal stresses are balanced solely by surface tension. In general, and especially when a surfactant is involved, dynamic interfacial phenomena contribute to the stress jump at an interface. These effects arise from surface-tension gradients due to mass transfer, interfacial elasticity, and interfacial viscosity (Levich 1962, Lucassen-Reynders 1981, Slattery & Flumerfelt 1982). Flumerfelt (1980) has extended the theory of drop deformation in steady shearing flows by incorporating a more general

constitutive equation for the surface stress and has shown that Cox's solution is unaltered to zero order in drop deformation if the viscosity ratio λ is replaced by

$$\lambda' = \frac{\mu^*}{\mu} + \frac{4\varepsilon}{5\mu a} + \frac{6\kappa}{5\mu a} + N_m, \tag{2}$$

where ε is the intrinsic surface shear viscosity, κ the intrinsic surface dilatational viscosity, and N_m the effective increase in the latter quantity stemming from mass-transfer-induced variations in surface tension along the drop interface. The influence of a viscous interface parallels that of drop-phase viscosity; both result in finite tangential stress components at the interface. Interfacial effects, as measured by λ', increase with decreasing drop size. Recognizing that the result in Equation (1) only depends upon the zero-order solution, we obtain the zero-shear viscosity when λ' replaces λ. The $O(\phi_d)$ coefficient for the effective viscosity of a suspension of inviscid bubbles varies from 1 to 5/2 as λ' varies from 0 to ∞, and the interface ranges from completely mobile to completely immobile, or "rigid." However, this analogy between λ and λ' does not carry over to first-order solutions in drop deformation.

Shear properties of dilute gas-bubble suspensions represent special cases of liquid-liquid emulsion theories, which assume incompressible flow. Taylor (1954) analyzed bubble expansion in an unbounded, otherwise quiescent fluid to determine the dilatational (bulk or expansion) viscosity μ' of a dilute gas-bubble suspension. Chen & Acrivos (1978) accounted for bubble-pair interactions and computed the first correction for nondilute concentrations. The primary contribution to μ' from the intrinsic interfacial dilatational viscosity κ has been obtained by Edwards (1987). The equation for μ' is

$$\mu' = \mu\left[\frac{4}{3\phi_d}\left(1 + \frac{\kappa}{\mu a}\right) - 1.733\right]. \tag{3}$$

For the purpose of evaluating various theoretical frameworks, it is interesting to note that Prud'homme & Bird (1978) employed a "cell" model and found the last term, due to interaction, to be -1.

For dilute emulsions, non-Newtonian effects arise from interactions between droplets and the external flow. By contrast, the shape of bubbles in static foam is largely determined by neighbors, and non-Newtonian behavior even occurs when viscous forces are absent. For these and similar reasons, there are striking differences between the rheology of foams and dilute gas-bubble suspensions.

EXPERIMENTAL OBSERVATIONS OF FOAM FLOW

Experimental difficulties associated with the systematic measurement of foam flow are both obvious and subtle, and they fall into two categories: those due to the physical nature of these structured fluids, and those due to rheological complexity. An outstanding physical characteristic of foam—its natural tendency to minimize free energy by reducing surface area—favors the bubble size to increase with time. Instability of the thin films due to inadequate surfactancy and related physicochemical mechanisms leads to film rupture and resultant bubble coalescence. Cheng & Natan (1986) have reviewed other degradation mechanisms that do not pertain to film stability but affect foam texture, which loosely refers to liquid content and cell-size distribution. Liquid drainage through foam due to gravity can cause temporal and spatial variations in the structure of foam as measured on the macroscale. Pressure differences across thin liquid films, due to their finite mean curvature, provide a driving force for gas diffusion between cells, especially in a polydisperse foam. This diffusion also causes bubble size to increase with time.

These stability considerations and the influence of foam-generation method and rate upon texture reinforce the need to characterize foam structure in rheological investigations. While all experimental studies report the liquid content of foams considered, few report cell size, and fewer yet its distribution. The degradation mechanisms already discussed can be suppressed substantially in liquid-liquid emulsions. This and the necessity to quantify structure and maintain it throughout the course of sometimes tedious measurements have led some investigators (Princen 1985, Princen & Kiss 1986, Yoshimura et al. 1987) to exploit the rheological similarity between foams and concentrated liquid-liquid emulsions. With the exception of compressibility, the analogy is excellent at low deformation rates, where interfacial phenomena determine rheological response. Some of the salient features of foam rheology to be described are most easily quantified with emulsions

Sibree (1934) showed that foam is highly viscous and shear thinning. Subsequent studies confirm this, even when the surfactant solution is Newtonian and of low viscosity, such as aqueous soap solutions. The shear-rate dependence of viscosity must be measured in so-called viscometric flows. Theory and practice governing the measurement of viscometric functions have been discussed by Coleman et al. (1966), Walters (1975), Schowalter (1978), Tanner (1985), and Bird et al. (1987). Loosely speaking, flow in tubes and rotational Couette devices is viscometric under proper conditions, while flow through contractions (where the deformation rate of a fluid element varies with time) is not.

Quite general methods for reducing data from viscometric flows exist; for example, in tube flow the variation with shear rate of both viscosity and wall-slip velocity can be determined from measurements of pressure drop and volumetric flow rate for tubes of different diameter (Mooney 1931). In general, these reduction methods are not parameter-fitting schemes that require prior knowledge of the explicit functional forms involved. But they do presume the fluid to be homogeneous and the flow to be incompressible, so foam dilatation must be minimal when the viscosity function is measured. A frequently cited analysis is claimed to correct for compressibility in capillary viscometry (David & Marsden 1969); however, it is internally inconsistent and cannot be justified (M. S. Kuntamukkula, personal communication).

Employing due caution, we can identify the salient features of foam rheology. Merely to call foam highly viscous is an understatement, because foam possesses a yield stress τ_y below which the deformation rate is zero and, therefore, the viscosity is infinite. When the shear stress τ exceeds the yield stress, the shear-rate-dependent viscosity $\mu_f(\dot{\gamma})$ can be represented by

$$\mu_f(\dot{\gamma}) = \tau_y/\dot{\gamma} + \mu_p(\dot{\gamma}), \qquad (\tau > \tau_y) \tag{4}$$

where $\mu_p(\dot{\gamma})$, often confused with *the* viscosity, is a constitutive function that depends upon shear rate. The Bingham-fluid model, with μ_p constant, is the most familiar form of Equation (4); other viscoplastic fluid models have been surveyed by Bird et al. (1982).

Barnes & Walters (1985) just considered the yield stress to be a convenient empiricism for representing the viscosity function over the shear-rate range of measurements. Strictly speaking, this range never includes zero. They conjectured that accurate measurements at lower shear rates will always disprove the existence of a yield stress, which "only defines *what cannot be measured.*" Caution is warranted because many yield-stress values reported for foams are just parameters obtained by fitting steady-flow data. Direct methods of yield-stress measurement rely upon assertions like "no flow was observed" below a critical shear stress; these statements must always be qualified, since the duration of observations and experimental sensitivity is finite. While recognizing the inadequacy of experiment to prove the existence of a yield stress, we assert that foam does have a yield stress and base this upon reasonable experimental evidence and the predictions of micromechanical models.

Early evidence of yield-stress phenomena in foams is due to Blackman (1948) and to measurements by Penney & Blackman, as described by Matalon (1953). Princen (1985) has conducted systematic measurements of the yield stress for concentrated emulsions. Many features of the data are represented by $\tau_y = \sigma\phi_d^{1/3}F(\phi_d)/\langle R\rangle$, where σ is surface tension, $F(\phi_d)$

an experimentally determined function, and $\langle R \rangle$ a measure of the mean bubble size. The function $F(\phi_d)$ increases by over an order of magnitude with increasing dispersed-phase volume fraction ϕ_d for the range $0.75 \lesssim \phi_d \lesssim 0.98$—*the yield stress is a strong function of liquid content.* Yoshimura et al. (1987) use the same emulsions but different experimental techniques and measure yield-stress values consistent with Princen. It is significant that their methods include constant-stress rheometry, the same technique used by Barnes & Walters (1985) to show that certain polymer solutions probably do not possess a yield stress at all, even though finite values are inferred from less sensitive measurements.

The rheological complexity of foam goes beyond shear-rate-dependent viscosity, the existence of a yield stress, and other non-Newtonian characteristics that can, in principle, be described by a constitutive relation for the bulk foam. "Slip at the wall" is another curious characteristic of foam flow. This slip, however, is merely a convenient macroscale description of the wall boundary condition, whose envisioned cell-level mechanism depends upon the existence of a thin fluid layer that does not itself slip but wets the wall and lubricates the foam flow. In steady, fully developed rectilinear flows, the slip velocity u_s can be expressed as a function of the wall shear stress τ_w according to

$$u_s = \psi_w(\tau_w)\tau_w, \tag{5}$$

where $\psi_w(\tau_w)$ is the slip coefficient (Mooney 1931) or wall fluidity (Princen 1985). There is experimental evidence for tube flow and rotational Couette flow [Siehr 1938, Penney & Blackman (as reported by Matalon 1953), Wenzel et al. 1970, Princen 1985] that the wall fluidity can vanish below finite values of τ_w (called the slip yield stress τ_{sy}). If the walls are smooth enough, a shear-stress range can exist where $\tau_{sy} < \tau_w < \tau_y$, and the foam is transported entirely by plug flow. This plug flow has also been reported by Beyer et al. (1972), Kraynik (1982), and Thondavadl & Lemlich (1985). When experiments are conducted with smooth transparent tubes so that it is possible to observe bubbles near the wall, no relative motion between adjacent bubbles is apparent below the yield stress. This is also true if a somewhat larger marker bubble is injected at the wall. By increasing the flow rate until relative motion of the marker and surrounding bubbles is observed, an estimate of foam yield stress can be obtained. Consistent with other measurements, the yield stress decreases with increasing liquid content (Kraynik 1982).

Systematic measurements that include the yield stress, slip at the wall, and the viscosity function of foam above the yield stress have not been reported; thus, limited information on the functional form and structural dependence of $\mu_p(\dot{\gamma})$, the last term in Equation (4), is available. Many

qualitative features of foam rheology may be attributed to the yield stress; for example, if we neglect $\mu_p(\dot{\gamma})$, the foam viscosity is given by $\mu_f = \tau_y/\dot{\gamma}$. This accounts for shear thinning and the effects of cell size and liquid content. Foam-viscosity data are sometimes fitted to the familiar power law $\mu_f = m\dot{\gamma}^{n-1}$, where m and n are constant parameters. When n is significantly greater than zero, viscous contributions beyond the yield stress are indicated; for example, Thondavadl & Lemlich (1985) report $n = 0.61$.

The slip, yield stress, and shear thinning associated with foam flow in tubes determine the qualitative velocity profile shown in Figure 1. To account for compressibility, Beyer et al. (1972) assumed that Bingham-fluid parameters and wall fluidity depend upon the local gas volume fraction (often called quality), which is related to local pressure through the ideal gas law. Their empirical model incorporates major features of foam rheology into calculations of foam flow in tubes and annuli. Mahalingam et al. (1975) used the data of Wenzel et al. (1967, 1970) to predict velocity profiles for incompressible flow in tubes. The foam viscosity is fitted to the Casson and Hershel-Bulkley models for viscoplastic fluids.

MICROMECHANICAL MODELS OF FOAM RHEOLOGY

Early Models

Empirical correlations of foam-flow data are of limited predictive value when the connection between structure and rheology is lacking. Until recently, the only attempt to relate foam viscosity to structure was a heuristic model for concentrated emulsions (Hatschek 1911, 1913), which

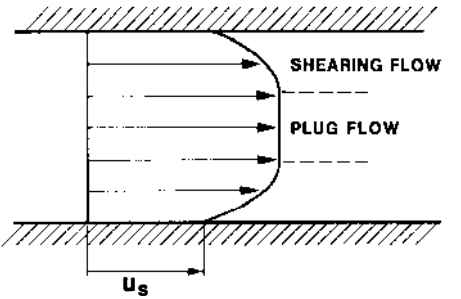

Figure 1 Velocity profile for fully developed flow of bulk foam in a tube. Three regions are illustrated: the solid-like plug region in which the shear stress does not exceed the yield stress and foam viscosity is infinite; the region of shearing flow in which the shear stress exceeds the yield stress and foam viscosity is finite; and the wall region in which the macroscopic foam velocity approaches a finite slip velocity u_s. In the absence of the second region, foam is transported entirely by plug flow due to slip.

has been applied to foams (Sibree 1934). Hatschek assumed that large shear rates distort the dispersed phase into parallelepipeds, which arrange into layers that slide relative to one another. Under the assumption of immobile interfaces, viscous dissipation in the liquid films between layers is large. The predicted foam viscosity $\mu_f/\mu = (1-\phi_d^{1/3})^{-1}$ increases with ϕ_d, the only structural parameter to appear. This qualitative dependence upon ϕ_d is observed experimentally but can also be attributed to the variation of yield stress with liquid content.

Assuming that liquid foam supports stress like a solid, Derjaguin (1933) analyzed its linear elastic behavior. The foam is considered to be a collection of randomly oriented, planar films whose deformations follow the imposed strain field, i.e. the deformations are affine. The predicted shear modulus is $G = 4\sigma S/15 \approx 8\sigma/5d_{32}$, where S is the surface area per unit volume, which is inversely related to cell size (e.g. $S \approx 6/d_{32}$, where d_{32} is the Sauter or surface-volume mean bubble diameter). Derjaguin also showed that the capillary pressure of foam, which is the difference between internal bubble pressure and external pressure, is given by $P_c = 2\sigma S/3$. It is important to recognize that affine film deformation is a kinematic hypothesis that implicitly neglects connectivity of the film network and therefore does not ensure equilibrium at the film junctions. Stamenovic & Wilson (1984) have indicated that the shear modulus is overestimated when the equilibrium configuration of the foam is not provided, a limitation that applies for affine shear deformations.

Spatially Periodic Models: Statics

Hatschek and Derjaguin address separately the viscous and elastic characteristics of foam. Neither approach can predict a yield stress or be generalized to reveal the true viscoelastic nature of these materials. Both treatments of three-dimensional structure are superficial; however, we have seen that a rigorous description of undeformed structure itself is rather involved. Suffice it to say that progress in developing micromechanical theories for foam rheology has been restricted to two-dimensional representations of foam structure and, moreover, to perfect order, except for the notable contributions of Weaire and associates (Weaire & Kermode 1983, 1984, Weaire & Rivier 1984, Weaire et al 1986, Weaire & Fu 1988).

An idealized foam structure for monodisperse bubbles was proposed by Princen (1979) and is shown in Figure 2. The hexagonal coordination minimizes surface free energy. Cell orientation is expressed by the angle θ, which is taken relative to the x-axis of a Cartesian coordinate system (x,y). Characteristic dimensions are the cell size a, the film thickness h, and the Plateau border curvature r. As a result of capillarity, the latter is responsible for lower pressure in the Plateau borders relative to that in the

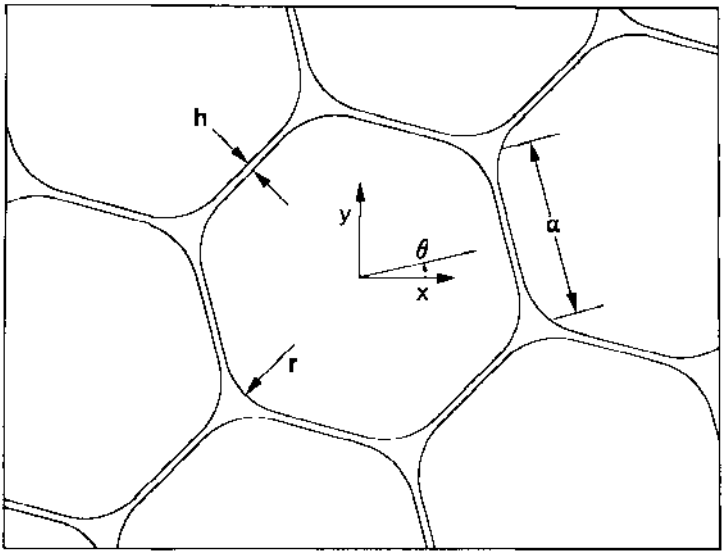

Figure 2 The equilibrium structure of an idealized two-dimensional foam showing films of finite thickness h, Plateau borders of uniform curvature r, the characteristic cell size a, and cell orientation angle θ.

bubbles. There is a pressure jump across the flat gas-liquid interfaces because of disjoining pressure, a quantity proposed by Derjaguin (1955) to describe the collective fluid microstructure forces in thin films due to molecular, ionic-electrostatic, and steric interaction effects. A positive disjoining pressure prevents all liquid from draining into the Plateau borders, is required for film stability, and depends upon the presence of surface-active species. In equilibrium, capillary pressure in the Plateau borders and disjoining pressure Π in the flat films are balanced, i.e. $\sigma/r = \Pi$. An explicit dependence upon film thickness $\Pi(h)$ is needed to determine the relative distribution of liquid between the Plateau borders and films. Teletzke and coworkers (Teletzke 1983, Teletzke et al. 1987a,b) have discussed the role of fluid microstructure forces in thin-film fluid mechanics and indicated length scales over which various contributions to disjoining pressure operate. These dimensions are in the range $1–10^3$ nm, so the proportion of liquid in the films can be very small for typical values of surface tension and bubble size.

Princen (1983) analyzed static deformations of these "liquid honeycombs" for simple shear and a particular cell orientation. Some essential features of this analysis were independently proposed by Prud'homme (1981). Figure 3 illustrates the variation in foam structure with shear strain

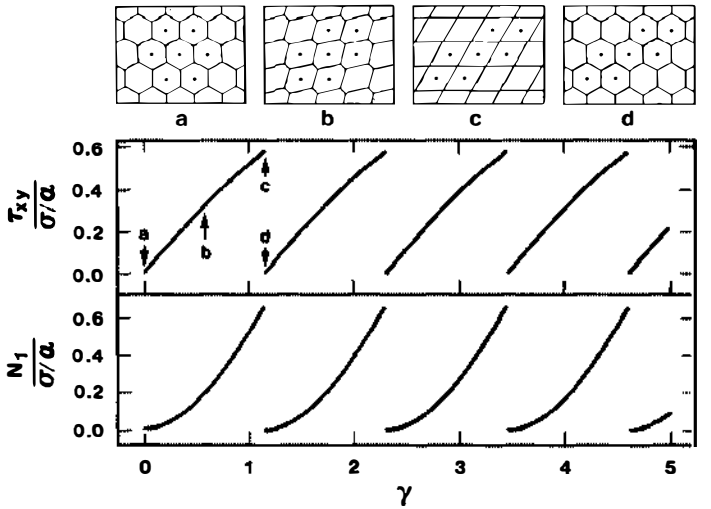

Figure 3 The Princen-Prud'homme model showing the variation with shear strain γ of foam structure and the corresponding shear stress τ_{xy} and first normal-stress difference $N_1 = \tau_{xx} - \tau_{yy}$ for simple shear with $\theta = 0$ and $\phi_d \to 1$: (*a*) undeformed network, $\gamma = 0$; (*b*) $\gamma = 3^{-1/2}$; (*c*) coalescence of film junctions (Plateau borders), $\gamma = 2(3^{-1/2})$; and (*d*) separation of junctions, $\gamma = 2(3^{-1/2})$, resulting in neighbor switching and, for this cell orientation, completion of the strain cycle.

γ when $\phi_d \to 1$; this is referred to henceforth as the Princen-Prud'homme model. When surface tension is uniform, three films continue to meet at equal angles of $2\pi/3$ until the critical strain $\gamma_c = 2(3^{-1/2})$, where four films meet, is reached. This marginally stable structure, which is associated with coalescence of two neighboring Plateau borders, balances surface-tension forces but does not minimize surface energy. The separation of junctions and the unique reorganization of films provide a stable structure with reduced interfacial area and identical cell midpoints. Kraynik & Hanser (1986, 1987) have called this separation process disproportionation, which is an unjustified and perhaps confusing label, since it refers to another thin-film phenomenon. Fortuitously, each coalescence and separation sequence, also referred to as "hopping," results in a structure that is identical to the rest state to within a translation of cells; however, this is only true for the specific cell orientation chosen. The shear stress, shown in Figure 3, is a periodic function of strain, and the maximum shear stress $\tau_{yc} = \sigma/a3^{1/2}$ has been interpreted as a yield stress.

Hopping provides an idealized micromechanical mechanism for yield behavior and flow on the macroscale—the relative separation of cells corresponds to switching of neighbors. Ashby & Verrall (1973) have noted

a fundamental topological feature of neighbor switching—it permits unbounded, permanent deformations on the macroscale while the cell distortion remains bounded. They observed neighbor switching in concentrated emulsions flowing between closely spaced, parallel glass plates. Similar qualitative observations of foams flowing near the wall of large rectangular ducts have been described by Wenzel et al. (1967).

Princen (1983) also accounted for finite liquid content in a micromechanical model of foam. The important role of Plateau borders is reemphasized for the case $h/r \to 0$, where the films are stabilized by disjoining pressure at vanishing thickness. Plateau borders of finite size require another film configuration (the so-called Mode II) to represent coalesced borders, as shown in Figure 4. Mode I refers to situations where individual Plateau borders and films are distinct. Princen determined the evolution of shear stress and of foam structure with increasing shear strain over the volume-fraction range $3^{1/2}\pi/6 \approx 0.9069 \leqq \phi_d < 1$. The lower limit on ϕ_d corresponds to maximum packing of cylindrical bubbles. Typical stress-strain curves for various ϕ_d are provided in Figure 5. The yield stress identified as τ_{yc}, the maximum shear stress, increases with ϕ_d. Mode I → Mode II → Mode I transitions occur for all stress-strain curves shown—some curves possess turning points. Curves corresponding to $\phi_d < \phi_d^* \approx 0.95$ are without turning points and are antisymmetric about the cycle midpoint $\gamma = 3^{-1/2}$, while those with turning points are not. For volume fractions below ϕ_d^*, stress-strain curves and variations in foam structure—in particular, Mode II → Mode I transitions—are smooth. Above ϕ_d^*, abrupt changes in stress and structure coincide with the turning point for increasing strain. While the Plateau border structure just prior to an abrupt transition is always Mode II, the structure following transition can be either Mode II or, for large ϕ_d, Mode I. When surface-tension forces dominate viscous forces in the slow shearing flow of foam, tran-

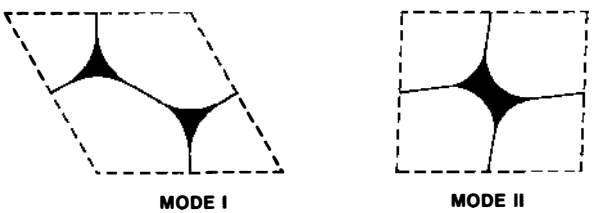

Figure 4 Typical repeating elements of foam structure with finite Plateau borders. The distinct Plateau borders, which characterize Mode I configurations, eventually coalesce with increasing strain and form a Mode II configuration. Adapted, with permission, from Princen (1983).

sitions involving turning points will be very rapid on the time scale defined by the shear rate and therefore cannot be considered quasi-static.

It is important to study rheology in flow types other than simple shear (e.g. extension). Khan & Armstrong (1986) have provided a theoretical framework for treating arbitrary homogeneous deformations, for which the deformation gradient tensor $\mathbf{E}$ does not depend upon position. They explicitly recognize that the motion of bubble centers and film midpoints is affine when the foam structure is perfectly ordered. When motion is affine, the displacement of a material point χ is given by the transformation $\chi' = \mathbf{E} \cdot \chi$, where χ' is the location at time t of χ, and the Cartesian components of $\mathbf{E}(t)$ are given by $E_{ij} = \partial \chi_i' / \partial \chi_j$. Analogous kinematics has been described by Adler & Brenner (1985) within the context of highly ordered suspensions and applies to spatially periodic media of quite general

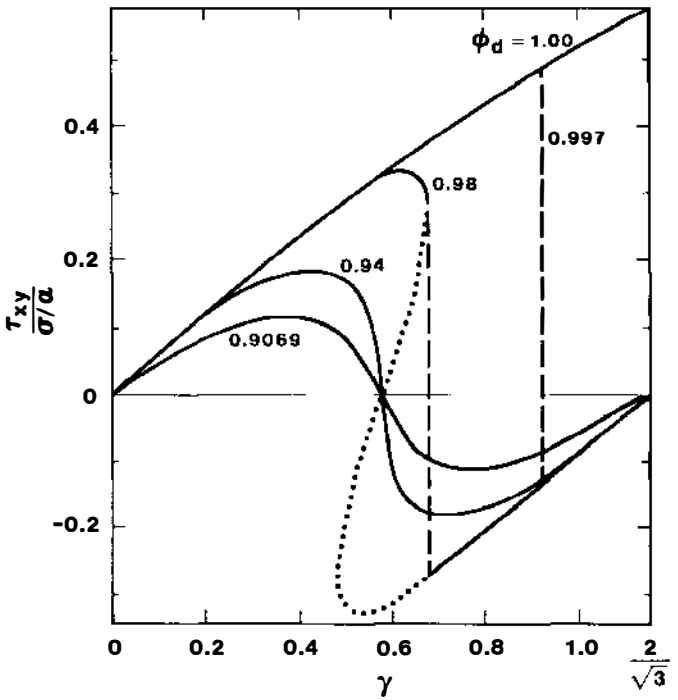

Figure 5 Shear-stress vs. shear-strain curves corresponding to two regimes of dispersed-phase volume fraction ϕ_d with $\theta = 0$ and $h \to 0$. When $\phi_d < \phi_d^* \approx 0.95$, the shear stress is antisymmetric about $\gamma = 3^{-1/2}$ and Mode II $\to$ Mode I transitions are smooth. When $\phi_d > \phi_d^*$, Mode II $\to$ Mode I transitions are abrupt, as indicated by the dashed line; the dotted line (shown only for $\phi_d = 0.98$) is the solution beyond the turning point that is inaccessible when strain is increasing. Adapted, with permission, from Princen (1983).

description. Proponents of spatially periodic theories recognize that the order imposed upon the structure is highly artificial with few, if any, examples in nature. This drawback must be weighed against the rigorous mathematical formulation and tractability afforded by the approach, as well as the insights provided by the predictions.

Spatial periodicity reduces the physical domain of interest to a unit cell that typically contains three half-films and a Plateau border, as shown in Figure 6. Let the center of a Plateau border and the midpoint of an adjacent film determine a vector $\mathbf{g}_i$. When $\phi_d \approx 1$, $\mathbf{g}_i$ represents the length and orientation of a half-film. The imposed macroscopic deformation determines the motion of the film midpoints, and the nonaffine junction displacement is governed by a balance of film tensile forces. For static deformations, which only account for uniform surface tension, the equilibrium relation reduces to algebraic equations expressing equal film angles. Khan & Armstrong (1986) considered simple shearing of arbitrarily oriented cells, with affine displacements given by $\Delta = \chi' - \chi = (\gamma y, 0)$. The shear stress and first normal-stress difference up to the yield point are given by

$$\tau_{xy} = (\sigma/a3^{1/2})\gamma(1+\gamma^2/4)^{-1/2} \quad \text{and} \quad N_1 = \tau_{xx} - \tau_{yy} = \gamma\tau_{xy}. \tag{6}$$

Their analysis for planar extension, where $\Delta = (x(e^{+\varepsilon}-1), y(e^{-\varepsilon}-1))$, determines the tensile stress

$$\tau_{xx} - \tau_{yy} = 4(\sigma/a3^{1/2}) \sinh(\varepsilon), \tag{7}$$

where ε is the Hencky strain measure. These stresses do not depend upon the initial orientation of the cells—that is, *the nonlinear elastic moduli are*

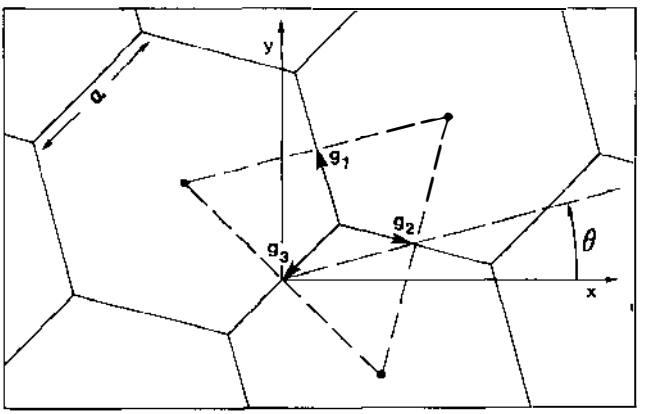

Figure 6 Schematic of an idealized foam structure showing the unit cell and half-film vectors $\mathbf{g}_i$.

isotropic below the yield point. Other implications of this are discussed by Khan (1987). The yield strain and corresponding yield stress do depend upon θ, so a unique value for τ_{yc} is not predicted. These equations for the nonlinear elastic stresses also apply for finite liquid content as long as Plateau borders do not coalesce, i.e. as long as the structure remains Mode I.

For comparison, if the deformation of complete films in an arbitrarily oriented two-dimensional foam is assumed to be affine, as in the three-dimensional analysis of Derjaguin (1933), the linear shear modulus is isotropic and given by $G = 3^{1/2}\sigma/2a$, which is a factor of 3/2 greater than that predicted by Equation (6). However, unlike the results of Khan & Armstrong (1986), isotropy is not maintained beyond the linear region.

Princen (1983) evaluates the shear stress by projecting the tension in the initially vertical film onto the shear plane, which is convenient for the particular cell orientation chosen. Khan & Armstrong (1986) show that work-energy equivalence can be used to determine stress, e.g. shear stress is given by $\tau_{xy} = \sigma\, \partial S/\partial\gamma$, where S is the surface area per unit volume; however, all information on the normal stresses is lost owing to the scalar nature of the method. The complete instantaneous stress tensor $\boldsymbol{\tau}$ for the foam can be derived from a volume average of the local stress tensor $\boldsymbol{\tau}'$ over the unit cell (Batchelor 1970, Adler et al. 1985, Khan & Armstrong 1986). When $\phi_d \to 1$ and only surface tension and bubble pressure P_b are considered, this provides

$$\boldsymbol{\tau} = -P_b\mathbf{I} + \frac{8\sigma}{3^{3/2}a}\sum_{i=1}^{3} g_i \mathbf{p}_i\mathbf{p}_i, \tag{8}$$

where g_i is the magnitude of $\mathbf{g}_i$ and both are scaled by a, and $\mathbf{p}_i = \mathbf{g}_i/g_i$ is a unit vector parallel to the ith film. A spatially periodic framework explicitly recognizes the inherent position and time dependence of the cell-level motion; therefore, the evaluation of *global* rheological properties, which are relevant to steady flows, requires averaging the instantaneous stress over time or, equivalently, over strain

$$\langle\boldsymbol{\tau}\rangle = \frac{1}{\mathscr{T}}\int_{\mathscr{T}} \boldsymbol{\tau}\, dt. \tag{9}$$

The global properties of the medium are properly represented when the time interval $\mathscr{T}$ is equated to the period of the motion (Adler et al. 1985, Kraynik & Hansen 1986).

The periodic variation of stress and structure with strain is readily inferred when $\theta = 0$, as in the Princen-Prud'homme model. Kraynik & Hansen (1986) identified the infinite set of discrete orientation angles that

admit strain-periodic behavior for simple shear. By accounting for the unique film rearrangement that is associated with any hopping process, the instantaneous stress can be determined for arbitrarily large strains when $\phi_d \to 1$. The global stress is only evaluated for strain-periodic orientations. It can be argued from energy-dissipation considerations that the global shear stress $\langle \tau_{xy} \rangle$ for very slow flows can also be identified as a yield stress. This quantity differs from τ_{yc} but, like it, varies with θ. Curiously, the physical appeal of the cell orientation originally chosen by Princen for simple shear cannot be justified on energy grounds because the global shear stress for $\theta = 0$ is the largest of any evaluated by Kraynik & Hansen. They also demonstrated the existence of strain-periodic orientations for planar extensional flow, which has been overlooked; complete analytical solutions describing the necessary and sufficient conditions have been obtained (Kraynik 1986). These results permit the evaluation of global tensile stresses and extensional viscosity.

Although global shear stress was not reported by Princen (1983), it vanishes for those cases not involving turning points, i.e. $\phi_d < \phi_d^*$. Under those conditions, the elastic strain energy is symmetric and completely recovered over the cycle (Khan 1985). The vanishing of global stress in the quasi-static regime corresponds to fluid-like behavior. Yet, for small strains below the yield point, the instantaneous stress is finite, corresponding to solid-like response. This dual character is peculiar and differs from Bingham-fluid behavior, in which the shear stress approaches a finite yield stress for slow flow.

Spatially Periodic Models: Viscous Effects

Cell-level viscous flow is a time-dependent free-surface problem. Many fundamental issues involving these fluid motions are unresolved, even when constraints imposed by idealized structure are accepted.

If we assume all liquid to be in the thin films, which either drain freely or do not drain at all, viscous effects can be estimated for simple shearing flow with velocity $\mathbf{v} = (\dot{\gamma} y, 0)$, cell orientation $\theta = 0$, and liquid volume fraction ϕ small but finite. The variation of structure with strain is assumed to be quasi-static, and the film-level flow is taken to be quasi-steady planar extension. For freely draining films, the instantaneous film thickness and extension rate are uniform throughout the foam. The estimated global shear stress fits the Bingham-fluid model with $\tau_y = 0.31\sigma/a$ and $\mu_p \approx 0.026\phi\mu$. Khan & Armstrong (1986) consider nondraining films, which do not exchange liquid with their neighbors and require the instantaneous film thickness and extension rate to vary between the films. They predict much larger viscous effects: $\mu_p \approx 13\phi\mu$.

A quasi-static approximation, which uncouples foam structure and vis-

cous flow, constrains rheological response. The coupling is responsible for many striking characteristics of fluids with structure. Kraynik & Hansen (1987) and Khan & Armstrong (1987) assume nondraining films and develop an ad hoc model to depict the strong interaction between structure and viscous forces. The nondraining limit corresponds to large drag forces resisting flow along the thin films. This assumption also provides a mechanism for the net tension in a film to differ from its neighbors, because respective stretch rates can vary, not only in magnitude but also in sign. The tensile force along the ith nondraining film is given by

$$\mathbf{F}_i = 2\sigma[1+(3^{1/2}/4)\phi\,\mathrm{Ca}\,\dot{g}_i/g_i^2]\mathbf{p}_i, \tag{10}$$

where $\mathrm{Ca} = \mu a\dot{\gamma}/\sigma$ is the capillary number, and $\dot{g}_i$ denotes the time derivative of g_i, with time scaled by the macroscopic deformation rate $\dot{\gamma}$. A force balance at the junction, $\sum_{i=1}^{3}\mathbf{F}_i = \mathbf{0}$, provides a set of coupled nonlinear ordinary differential equations that determine the film vectors $\mathbf{g}_i$ given the film midpoint motion for the imposed flow. Junction coalescence is assumed to occur whenever a film's length becomes less than its thickness, i.e. $g_i^2 < 3^{1/2}\phi/8$. Plausible initial conditions for junction separation and fast growth of the new film are then prescribed. The stress-strain curve that corresponds to the Princen-Prud'homme model with viscous effects, shown in Figure 7, illustrates the influence of film-level viscous flow when $\mathrm{Ca} = 4(3^{-1/2})$, $\phi = 0.01$, and $\theta = 0$. The asymptotic approach to periodic

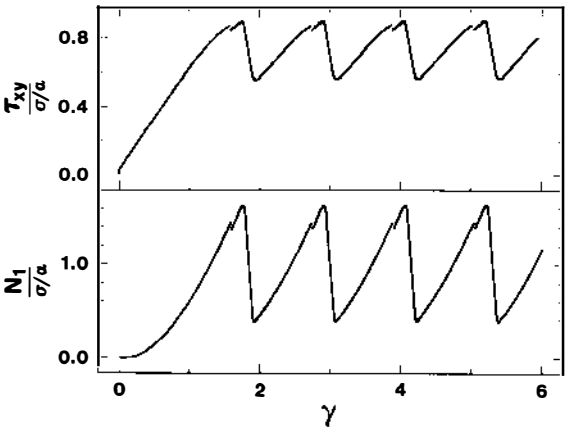

Figure 7 Variation with shear strain γ of the instantaneous shear stress τ_{xy} and first normal-stress difference $N_1 = \tau_{xx} - \tau_{yy}$ for simple shearing flow with $\theta = 0$, $\phi = 0.01$, and $\mathrm{Ca} = 4(3^{-1/2})$.

stress represents the spatially periodic analog of steady shearing flow. To within isotropic terms, the instantaneous stress tensor is given by

$$\tau = \frac{8\sigma}{3^{3/2}a}\left\{\sum_{i=1}^{3}\left[1+(3^{1/2}/2)\phi\,\mathrm{Ca}\,\frac{\dot{g}_i}{g_i^2}\right][g_i\mathbf{p}_i\mathbf{p}_i]\right\}. \tag{11}$$

Global material functions for simple shearing flow are shown in Figure 8 (Kraynik & Hansen 1987). The quasi-static regime, $\mathrm{Ca} \to 0$, determines a yield stress. The dashed curve represents the contribution of the surface-tension term in Equation (11) to the global shear stress. Its variation with capillary number reflects the rate dependence of foam structure. The remaining, viscous contribution to the shear stress is relatively small. The primary role of viscous forces is their influence upon instantaneous film length and orientation, which differs substantially from the quasi-static regime. The computed material functions terminate at a critical capillary number beyond which the stress does not converge to periodic behavior for very large strains, so the time average in Equation (9) is not meaningful. This is accompanied by large cell distortion and film thinning, which promotes film rupture. Thus, a plausible mechanism for shear-induced failure of foams is suggested. Interpreting Figure 8 literally, the shear-stress range that corresponds to steady shearing flow is relatively small.

Kraynik (1987) determined the linear viscoelastic response for this model. Complex interfacial rheology can be introduced into the analysis by using intrinsic interfacial parameters to represent Gibbs elasticity I and the interfacial viscosities κ and ε. The tension in a nondraining film is given by

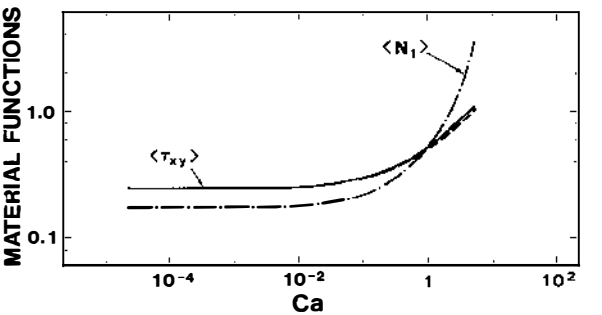

Figure 8 Material functions for simple shearing flow with $\theta = 0$ and $\phi = 0.01$: global shear stress $\langle\tau_{xy}\rangle$ and global first normal-stress difference $\langle N_1\rangle = \langle\tau_{xx}\rangle - \langle\tau_{yy}\rangle$. The dashed curve represents the contribution of the surface-tension term in Equation (11) to the global shear stress.

$$\mathbf{F}_i = 2\sigma\{1+N_G \ln(2g_i)+[N_S g_i^{-1}+(4g_i)^{-2}]\dot{g}_i\}\mathbf{p}_i, \tag{12}$$

where $N_G = \Gamma/\sigma$, $N_S = 3^{-1/2}(\kappa+\varepsilon)/\phi\mu a$, and $\dot{}$ denotes the time derivative, with time scaled by $3^{1/2}\phi\mu a/\sigma$. Restricting the analysis to small deformations eliminates the need to consider Plateau border coalescence. The predicted stress-relaxation modulus is given by

$$G(t^*) = \frac{\sigma}{3^{1/2}a(1+N_G)}(1+3N_G+2e^{-t^*}), \tag{13}$$

where time t^* has been scaled by $(3^{1/2}\phi\mu a+\kappa+\varepsilon)/(\sigma+\Gamma)$, the characteristic relaxation time. The stress-relaxation modulus $G(t^*)$, derived by considering arbitrary cell orientation with respect to the principal axes of strain for simple shear, is isotropic and consistent with a similar analysis for planar extension. Realistic qualitative behavior is captured by Equation (13); for example, a finite equilibrium shear modulus $G(t^* \to \infty)$ is indicative of the gel-like response of foam. The dependence of the material time scale upon parameters relating to texture, viscous flow, and dynamic interfacial properties evinces the complexity of foam rheology.

For freely draining films, dissipative effects do not appear in the linear regime because the variation in total film length is $O(\gamma^2)$. The corresponding response is purely elastic, with the stress-relaxation modulus the same as the static shear modulus $G = \sigma/a3^{1/2}$, consistent with Equation (6).

Assuming all of the liquid to be in the films and neglecting interfilm flow provides a tractable mathematical model for the interaction between cell structure and viscous flow, but film-level transport and foam structure are compromised when Plateau borders are neglected. Pacetti (1985) and Schwartz & Princen (1987) have proposed different models that incorporate Plateau borders.

Pacetti (1985) considered simple shearing flow and the initial cell orientation originally investigated by Princen (1983). The foam structure consists of Plateau borders with uniform curvature and flat films of uniform thickness that are stabilized by disjoining pressure. In effect, the thickness is permitted to vary slightly between films. This structure is consistent with quasi-static deformations, but the rapid separation of Plateau borders (Mode II → Mode I), for ϕ_d close to unity, is not. Recognizing this, Pacetti only considers volume fractions that produce stress-strain curves without turning points—recall that the corresponding Mode II → Mode I transitions are smooth, and therefore the flow can be considered quasi-steady. Within the limitations of a flat-film approximation, results are obtained for mobile interfaces, along which surface tension is uniform and shear stress vanishes in the films. Fluid exchange with the Plateau borders and

neighboring films is accounted for, and flow in the films is taken to be quasi-steady planar extension. Viscous tractions arise from the small variations in film thickness during a strain cycle. These variations are required to conserve liquid and balance border suction with disjoining pressure. The instantaneous shear stress is evaluated by a method that requires verification against a rigorous volume average; however, qualitative features predicted by the analysis should not be affected. The interfaces do not contribute to the global shear stress, and the viscous contribution is very small, consistent with our previous estimate for mobile films. The choice of conditions that are consistent with a quasi-steady approximation to viscous flow, for all times, is a unique and noteworthy feature of Pacetti's approach.

To incorporate viscous effects, Schwartz & Princen (1987) considered all liquid to be in the Plateau borders, except for a very small amount confined to immobile equilibrium films stabilized by the disjoining pressure. They analyzed viscous dissipation due to immobile films being drawn from or falling into the border. The quasi-static response of foam to time-periodic planar extension is considered, with the strain magnitude sufficiently small that adjacent Plateau borders do not coalesce. A particular orientation, with some films parallel to a macroscopic stretching direction, is analyzed. Their theory parallels the steady-state analysis of Mysels et al. (1959), who studied flow due to soap films moving relative to their borders. For slow speeds, the significant fluid flow and viscous forces are confined to a small transition region where the film enters the mouth of the Plateau border. Figure 9 illustrates the four regions of the film, which correspond to the Plateau border (a static meniscus), a transition region, a liquid-entrainment region, and an equilibrium thin (black) film. The exact film profile in the liquid-entrainment region depends upon

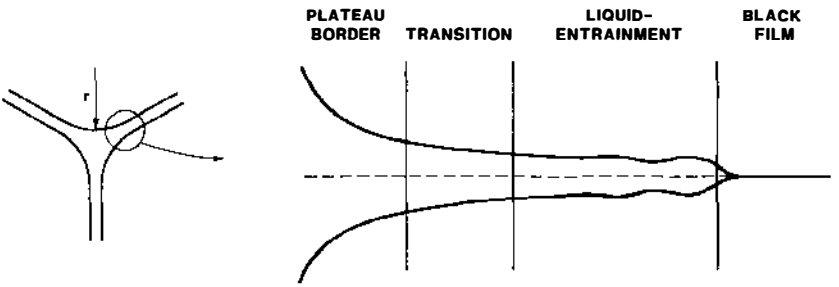

Figure 9 Schematic of the four film regions that are accounted for in the analysis of Schwartz & Princen (1987): the Plateau border, the transition region, the liquid-entrainment region, and equilibrium thin (black) film.

time and position, in contrast to steady-state analyses where it is uniform. The quasi-steady lubrication version of the Stokes equations applies to the transition region, where interfaces are nearly parallel, and leads to an ordinary differential equation for the film profile

$$\eta''' = (\eta - 1)/\eta^3. \tag{14}$$

Here η represents film thickness scaled to that in the liquid-entrainment region h^*_∞, primes denote differentiation with respect to the stretched film coordinate, which is fixed to the border $\xi = x(3\mathrm{Ca}^*)^{1/3}/h^*_\infty$, and Ca* is the capillary number based upon film speed (which is small). An asterisk indicates instantaneous quantities.

Equation (14) arises in the analysis of many free-boundary, visco-capillary-flow problems (Schwartz et al. 1986). It has been used to analyze coating flows (Landau & Levich 1942, Ruschak 1985), the soap-film withdrawal already mentioned, and the motion of long bubbles in small tubes (Bretherton 1961). Such model problems represent important features of viscous dissipation in bulk foams, their slip at the wall, and foam displacement in porous media. The techniques of matched asymptotic analysis are required to fully resolve flow in the transition zone, which must match conditions in both the border and liquid-entrainment regions (Park & Homsy 1984).

The instantaneous entrained-film thickness can be expressed as $h^*_\infty = 2r(3\mathrm{Ca}^*)^{2/3}P$, where $P = \eta''$ is the asymptotic curvature on the border side of the transition region evaluated in the stretched variables. A unique solution, $P = 0.6340$, is obtained when thin film is withdrawn from the border. However, the problem is underdetermined when film falls into the border (Mysels et al. 1959), and a one-parameter family of solutions corresponding to different values of P is possible. Schwartz & Princen exploit the temporal periodicity of both the imposed motion and the quasi-static evolution of foam structure to resolve the indeterminacy at any time. The viscous dissipation per unit cell per cycle is calculated, which they express as an effective foam viscosity $\mu_e \sim \mu\mathrm{Ca}^{-1/3}$, where Ca is based upon the apparent deformation rate of the foam during a cycle. The quantity μ_e can be compared with the Bingham viscosity parameter of previous estimates, for which $\mu_p \sim \phi\mu$. The effective viscosity μ_e is large for small capillary numbers and does not depend upon the liquid content of the foam. The relative strength of the dissipation mechanism proposed by Schwartz & Princen is due to the large magnitude of shearing in the thin transition regions whose interfaces are assumed to be immobile. The same assumption leads to Frankel's law for soap-film withdrawal: $H = 1.88\mathrm{Ca}^{2/3}(\sigma/\rho g)^{1/2}$, where H is film thickness, and the capillary number

is based upon film speed (Mysels et al. 1959). Mysels & Cox (1962) and Lyklema et al. (1965) have confirmed Frankel's law experimentally when film thickness is large enough to neglect disjoining pressure effects and surfactant solutions that provide an immobile interface are used.

The complete independence of effective viscosity on liquid volume fraction ϕ, predicted by Schwartz & Princen, should not carry over to the global contribution of dissipation to stress in steady shearing flows. This hypothesis assumes that the proportion of time spent in Mode I and Mode II is important and depends upon ϕ. Restricting attention to small strains avoids mode transitions and their fundamental role in foam flow. Focusing on smooth mode transitions offers a convenient approach to incorporating viscous effects into micromechanical theories. The eventual analysis of rapid transitions is essential to an improved understanding of foam rheology; however, the analytical and computational techniques required of that time-dependent free-boundary analysis, which couples viscous forces in adjacent films, represents a significant challenge.

The ideas of Princen and Schwartz suggest a point of departure for future studies of film-level flow, within the constraints of foam structure. Strictly speaking, their analysis applies when entrained film is much thicker than the equilibrium film thickness set by disjoining pressure. This restriction has been relaxed by Teletzke and coworkers (Teletzke 1983, Teletzke et al. 1987b), who extend the hydrodynamic film evolution equation to include fluid microstructure forces of molecular and colloidal origin. When a positive disjoining pressure, taken to decrease with film thickness, is included into a steady-state analysis corresponding to film withdrawal, a second, quasi-static regime appears for very small capillary numbers. The transition to this quasi-static regime, in which film tension and thickness take on their static values and dissipation vanishes rapidly, is very abrupt, occurring over a narrow range in capillary number that depends upon the length scale set by disjoining pressure. This transition has been observed experimentally by Lyklema et al. (1965).

The process of Plateau border coalescence and separation—fundamental to foam flow—is captured by spatially periodic models. The constraints imposed by ordered structure provide a convenient theoretical framework for investigating this fundamental mechanism, which in itself justifies spatially periodic theories. The hope, however, is that other predictions are not so hampered by constraints of perfect order as to render these analyses into mathematical exercises barren of physical content. One cannot rigorously choose between fact and artifact produced by these theories; instead, one must rely upon intuition and experience, proven enemies in the past. While the ultimate test of a theory is experiment, one can gain partial confirmation of spatially periodic models and probe their

limitations by comparing the resulting predictions with those for disordered media.

Statics of Disordered Two-Dimensional Foams

Khan & Armstrong (1987) have analyzed the static response of bidisperse, spatially periodic foams; however, entirely different methods are required for polydisperse systems that are highly disordered. Such techniques have been developed by Weaire & Kermode (1983, 1984), initially to study the role of intercellular diffusion in the temporal evolution of structure. This in itself is of interest because the rheology of foam depends upon its texture. Simulations of diffusion phenomena in foams can be compared with their experimental counterparts in two dimensions (Glazier et al. 1987) and three dimensions (Cheng & Lemlich 1985). The close analogy between foams and random cellular media of various origins has been reviewed by Weaire & Rivier (1984) and motivates broad interest in the subject.

Many will find the cellular structures analyzed by Weaire & Kermode to be a refreshing departure from the constraints of perfect order. One hundred cells that comprise a typical spatially periodic unit cell are shown in Figure 10. Various algorithms are employed to specify a random distribution of points that serve as the nuclei for a periodic Voronoi network. The Voronoi polygons, which possess straight sides and unequal film angles as shown in Figure 10, are adjusted to achieve an equilibrium rest state. The resulting disordered structure consists of cells with varying numbers of curved films. The second moment $\mu_2 = \sum_{n=3}^{\infty}(n-6)^2 f(n)$ of

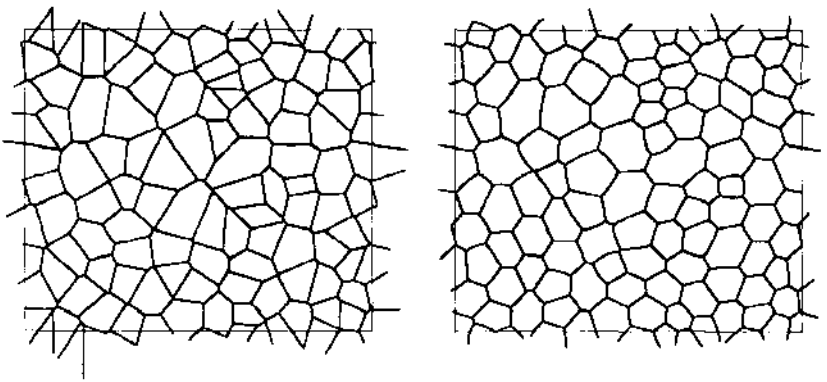

Figure 10 Typical disordered two-dimensional foam structure analyzed by Weaire & Kermode (1983, 1984) showing the unadjusted Voronoi polygons with straight sides and unequal film angles (on the left), and the relaxed structure in which three films meet at equal angles.

the number distribution of cell sides $f(n)$ is used as a measure of disorder. In Figure 10, this value is $\mu_2 \approx 1.00$.

The rheological studies are restricted to static planar extension and $\phi_d \to 1$. The tensile stress is evaluated by the energy method, i.e. $T = \tau_{xx} - \tau_{yy} = \sigma \partial S/\partial \varepsilon$. An iterative numerical scheme was developed to solve the system of algebraic equations determined by cell volume, equilibrium, and deformation constraints, along with an algorithm to specify the abrupt coalescence and separation of film junctions, which Weaire & Kermode refer to as a T1 process.

The initial study of mechanics by Weaire & Kermode (1984) considered periodic deformations large enough to require numerous T1 processes. Within the disordered medium, T1 events occur sporadically throughout. By contrast, two simultaneous T1 events are forced upon each and every monodisperse cell in the idealized case—the cells alternate between six and four sides. This perfect correlation of T1 events causes large discontinuities in stress and structure, as shown in Figure 3. However, the essentially uncorrelated T1 processes in disordered media result in fluctuations of diminished intensity in stress and structure. Presumably, on the macroscale, fluctuations vanish and stress-strain response becomes smooth when the population of the unit cell is sufficiently large and disordered.

Quantitative comparisons of the linear shear modulus G for disordered and ideal media are quite satisfying. Weaire et al. (1986) have computed G for several structures with μ_2 values up to 2.9 and report that a reduced modulus $G^* = \langle a \rangle G/2\sigma$ is relatively insensitive to disorder, decreasing slightly with μ_2. Here, the characteristic cell size is given by $\langle a \rangle^2 = N^{-1} \sum_{i=1}^{N} A_i$, where A_i is the area of the ith cell in a population of N cells. For a perfectly ordered system, the reduced modulus value is given by $G^* = 3^{1/4}2^{-3/2} \approx 0.465$. This represents an upper bound for all of their simulations and leads Weaire et al. to conjecture that it is a strict upper bound. Princen (1983, 1985) recommends correlating stress and modulus data with a characteristic cell size based upon the Sauter mean diameter $d_{32} = (\sum n_i d_i^3)/(\sum n_i d_i^2)$, where there are n_i bubbles of equivalent spherical diameter d_i. Neither $\langle a \rangle$ nor the two-dimensional counterpart of d_{32} is justified by analysis. Simulations could guide the experimentalist to an optimal choice of length scale.

Weaire & Fu (1988) have simulated complete stress-strain curves $T(\varepsilon)$ for ε up to about 1.2, various μ_2, and 64 cells per repeat. To a good approximation, the reduced tensile stress $T^* = \langle a \rangle T/2\sigma$ is a monotonically increasing function of strain, apart from fluctuations, and is fit by $T^* = T_\infty \tanh(2\varepsilon')$, where ε' is a linear strain measure given by $\varepsilon = \ln(1 + \varepsilon')$. The asymptotic value T_∞ is of order unity for all simulations.

Kraynik & Hansen (1986) have shown that ideal structure, with $\theta = \pi/12$, provides the simplest strain-periodic response in planar extension. The corresponding global average of $T^*(\varepsilon)$ is a lower bound for all the cases that Kraynik & Hansen consider and is comparable in magnitude to T_∞ computed by Weaire & Fu.

The agreement between ideal and disordered systems for both the linear moduli and global stress is very encouraging. It emphasizes the intrinsic value of simulations and substantiates the validity of properly interpreted spatially periodic theories. However, these favorable comparisons should be viewed as preliminary and require further study.

It is important to note that the concept of a yield stress is also supported by simulations of disordered foams.

SLIP AT THE WALL

Slip at the wall on the macroscale is a major feature of foam flow. Consider a conceptual model of the wall region consisting of a thin liquid film of uniform thickness h_e and viscosity μ. Assume that the slip velocity u_s is equal to the uniform velocity of the gas-liquid interface, which is immobile and translates with the average velocity of bubbles adjacent to the wall. If the slip velocity is given by $u_s = h_e\tau_w/\mu$, then the wall fluidity of equation (5) is simply $\psi_w = h_e/\mu$. Effective film thicknesses calculated from typical data can be as large as 10 μm but are usually smaller and vary with wall shear stress (Wenzel et al. 1970, Princen 1985, Thondavadl & Lemlich 1985). Wall slip is an appropriate boundary condition when $h_e \ll \mathscr{L}$, the macroscopic length scale of the flow.

A more realistic model of the wall region accounts for Plateau borders, as shown in Figure 11. At rest and neglecting gravity, the wall film-

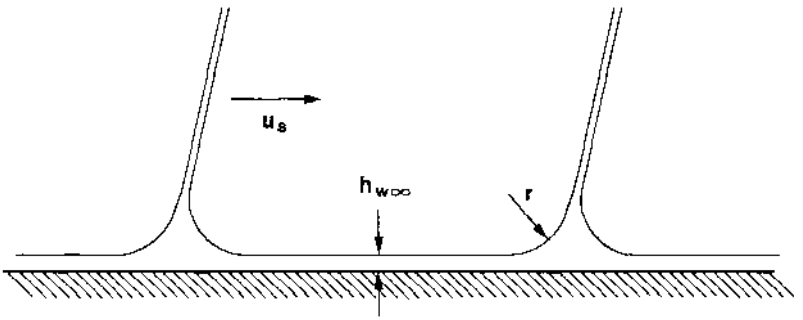

Figure 11 Schematic of the wall region when the continuous liquid phase completely wets the wall. Plateau borders with curvature r and thin liquid films of thickness $h_{w\infty}$ are shown.

thickness profile is determined by wetting effects that depend upon capillary pressure in the Plateau borders and disjoining pressure in the wall film $\Pi_w(h_w)$, which may differ from $\Pi(h)$ for films in the bulk foam. Mannheimer's (1972) experiments with concentrated emulsions show a strong influence of wall materials with different wetting characteristics on slip. Princen (1985) measured slip velocities for well-characterized series of emulsions and treated the walls to ensure complete wetting by the continuous phase. He measured the fractional area of static thin films adjacent to the wall, assumed that wall shear stress on the macroscale is determined entirely by shear flow in thin films with immobile interfaces, and calculated film thicknesses less than the corresponding values of h_e, e.g. 17 nm vs. 45 nm. In some cases, slip could not be measured below finite wall shear stresses of order 1 Pa, suggesting a slip yield stress whose origin Princen attributed to wall roughness. Thondavadl & Lemlich (1985) did not observe slip in rough pipes, whereas it was prevalent in smooth ones.

Wall slip on the macroscale can be related to foam structure and viscous flow near the wall by extending Bretherton's (1961) analysis, which describes the motion of large bubbles in small capillaries. Consider steady flow near the wall of a two-dimensional, monodisperse foam with immobile interfaces. Assume that the bulk foam moves in plug flow, i.e. $\tau_w < \tau_y$. Neglecting the liquid content of thin films in the bulk foam, the Plateau border curvature is given by $r/a = 2.84\phi^{1/2}$ (Princen 1979). The analysis of Teletzke and coworkers (Teletzke 1983, Teletzke et al. 1987b) could be used to relate the uniform thickness of entrained film, $h_{w\infty}$, to Plateau border curvature r and a capillary number based upon slip velocity, $Ca_s = \mu u_s/\sigma$. For $Ca_s \to 0$, the equilibrium wall film thickness is obtained from $\Pi_w(h_w) = \sigma/r$, given the functional form of disjoining pressure. Bretherton's solution, $h_{w\infty}/r = 2.12\ Ca_s^{2/3}$, which applies when $h_{w\infty} \gg h_{w\infty}(Ca_s \to 0)$ and $Ca_s \ll 1$, provides the following relation for the slip velocity:

$$Ca_s^{1/3} = 6.02a\phi^{1/2}\tau_w/\sigma f, \tag{15}$$

where $f = 1 - 3.28\phi^{1/2}$ represents the fraction of the wall covered by thin film. Equation (15) is in qualitative agreement with Princen's (1985) systematic measurements, which indicate that wall fluidity ψ_w increases with increasing wall shear stress, continuous-phase volume fraction, and drop size.

An interest in foam displacement in porous media motivated Hirasaki & Lawson (1985) to study flow in capillary tubes whose radius R is comparable to the equivalent spherical radius R_b of carefully generated uniform bubbles. To relate foam flow to structure, they proposed a quan-

titative model in which R_b/R is permitted to be large, $O(1)$, or small. Plug flow is assumed in the bulk-foam regime. The model incorporates an ad hoc modification of the Bretherton analysis to represent diffusion-induced surface-tension gradients; the interfacial mobility of the bubbles, which varies from perfectly mobile to immobile, depends upon the value of a single parameter. The corresponding special case of the Hirasaki-Lawson model is similar to Equation (15). The model of Hirasaki & Lawson captures a wide range of phenomena and motivates current systematic studies (G. M. Ginley & C. R. Radke, E. Herbolzheimer, J. Ratulowski & H. C. Chang, unpublished results) of dynamic interfacial effects whose origin may include both diffusion of surfactants and intrinsic properties such as interfacial viscosity. Falls et al. (1987) have applied the work of Hirasaki & Lawson to foam displacement in porous media, a currently active research topic in multiphase flow (e.g. Gauglitz 1986, Ransohoff 1986, Prieditis 1987).

COMPLEX FLOWS OF VISCOPLASTIC FLUIDS

Scalar material functions for foam viscosity and wall fluidity—specific forms of Equations (4) and (5), respectively—are sufficient to determine velocity fields for the steady rectilinear flows emphasized thus far. The analysis of complex flows with nonrectilinear streamlines requires constitutive equations of proper tensor character for the bulk fluid and, if slip is considered, the wall boundary condition. Since foams can be modeled as viscoplastic fluids if their viscoelastic character is neglected, the following two studies of viscoplastic fluids relate to complex flows of foam and illustrate the numerical simulation techniques required.

The work of Beris et al. (1985) is relevant to the particle-carrying capacity of foam. They apply finite element methods to analyze the creeping motion of a rigid sphere through a Bingham fluid, assuming no slip. The sphere moves in an envelope of fluid, whose shape depends upon the yield stress τ_y, when $2\tau_y \pi R_s^2/F \lesssim 0.143$, where R_s is the sphere radius and F is the applied force. The boundaries of the envelope include an outer yield surface and two inner yield surfaces due to unyielded "fluid" at the front and back of the sphere.

Tilton (1985) has also used finite elements to simulate steady creeping flow through a tube with a smooth axisymmetric constriction. Bingham and other viscoplastic fluids that slip at the wall are analyzed. A linear slip boundary condition, corresponding to constant wall fluidity ψ_w, is assumed and is given by

$$\mathbf{u}_s = \psi_w(\mathbf{n}\cdot\boldsymbol{\tau}\cdot\mathbf{t})\mathbf{t}, \tag{16}$$

where $\mathbf{n}$ is a unit vector normal to the wall and directed into the fluid, $\boldsymbol{\tau}$ is the stress, and $\mathbf{t}$ is a unit vector tangent to the wall. The solid-like plug associated with fully developed flow terminates prior to entering the constriction and reforms following it—a plug of finite radius cannot survive passage through the constriction because reversible elastic deformations of unyielded material are not accounted for.

CONCLUDING REMARKS

The experimental study of foam flow has been pursued for over half a century; by contrast, less than a decade has passed since the initial development of micromechanical theories for foam rheology. The collective data that predate the theories reveal many curious rheological features of foam, such as a yield stress and slip at the wall, which stem from foam structure and the physical characteristics of its constituents and interfaces. Current theories cannot provide definitive relationships between foam structure and rheology because they are restricted by two dimensionality in all cases and perfect order in most cases. Once the proper film-level mechanisms involving interfacial transport and viscous flow are incorporated into disordered two-dimensional models, the significant steps to three dimensions can be taken. Meanwhile, the current theories provide a rational basis for developing our intuition and reinforce the need for careful characterization of foam structure and systematic rheological measurements.

ACKNOWLEDGMENTS

This work was performed at Sandia National Laboratories and supported by the US Department of Energy under contract # DE-AC04-76DP00789. I am very grateful to N. E. Bixler, R. W. Flumerfelt, A. S. Geller, S. A. Khan, M. S. Kuntamukkula, D. F. McTigue, H. M. Princen, L. W. Schwartz, G. F. Teletzke, and D. Weaire for providing helpful comments.

Literature Cited

Adler, P. M., Brenner, H. 1985. Spatially periodic suspensions of convex particles in linear shear flows. I. Description and kinematics. *Int. J. Multiphase Flow* 11: 361–85

Adler, P. M., Brenner, H. 1988. Multiphase flow in porous media. *Ann. Rev. Fluid Mech.* 20: 35–59

Adler, P. M., Zuzovsky, M., Brenner, H. 1985. Spatially periodic suspensions of convex particles in linear shear flows. II. Rheology. *Int. J. Multiphase Flow* 11: 387–417

Ashby, M. F., Verrall, R. A. 1973. Diffusion-accommodated flow and superplasticity. *Acta Metall.* 21: 149–63

Assar, G. R., Burley, R. W. 1986. Hydrodynamics of foam flow in pipes, capillary

tubes, and porous media. In *Encyclopedia of Fluid Mechanics*, ed. N. P. Cheremisinoff, 3: 26-42. Houston: Gulf

Barnes, H. A., Walters, K. 1985. The yield stress myth? *Rheol. Acta* 24: 323–26

Batchelor, G. K. 1970. The stress system in a suspension of force-free particles. *J. Fluid Mech.* 41: 545–70

Beris, A. N., Tsamopoulos, J. A., Armstrong, R. C., Brown, R. A. 1985. Creeping motion of a sphere through a Bingham plastic. *J. Fluid Mech.* 158: 219–44

Beyer, A. H., Millhone, R. S., Foote, R. W. 1972. Flow behavior of foam as a well circulating fluid. *SPE 3986*, Soc. Pet. Eng., San Antonio, Tex.

Bikerman, J. J. 1973. *Foams.* New York: Springer-Verlag. 337 pp.

Bird, R. B., Armstrong, R. C., Hassager, O. 1987. *Dynamics of Polymeric Liquids, Vol. 1: Fluid Mechanics.* New York: Wiley-Interscience. 649 pp. 2nd ed.

Bird, R. B., Dai, G. C., Yarusso, B. J. 1982. The rheology and flow of viscoplastic materials. *Rev. Chem. Eng.* 1: 1–70

Blackman, M. 1948. On the transformation of "solid" foam to a "fluid" foam under shear. *Trans. Faraday Soc.* 44: 205–6

Bretherton, F. P. 1961. The motion of long bubbles in tubes. *J. Fluid Mech.* 10: 166–88

Chen, H.-S., Acrivos, A. 1978. The effective elastic moduli of composite materials containing spherical inclusions at non-dilute concentrations. *Int. J. Solids Struct.* 14: 349–64

Cheng, H. C., Lemlich, R. 1985. Theory and experiment for interbubble gas diffusion in foam. *Ind. Eng. Chem. Fundam.* 24: 44–49

Cheng, H. C., Natan, T. E. 1986. Measurement and physical properties of foam. In *Encyclopedia of Fluid Mechanics*, ed. N. P. Cheremisinoff, 3: 3–25. Houston: Gulf

Coleman, B. D., Markovitz, H., Noll, W. 1966. *Viscometric Flows of Non-Newtonian Fluids.* New York: Springer-Verlag. 130 pp.

Cox, R. G. 1969. The deformation of a drop in a general time-dependent fluid flow. *J. Fluid Mech.* 37: 601–23

David, A., Marsden, S. S. 1969. The rheology of foam. *SPE 2544*, Soc. Pet. Eng., Denver, Colo.

Derjaguin, B. V. 1933. Die elastischen Eigenschaften der Schäume. *Kolloid-Z.* 64: 1–6

Derjaguin, B. V. 1955. Definition of the concept of, and magnitude of the disjoining pressure and its role in the statics and kinetics of thin layers of liquids. *Colloid J.* 17: 191–97 (From Russian)

Edwards, D. A. 1987. *Surface rheology.* PhD thesis. Ill. Inst. Technol., Chicago. 196 pp.

Falls, A. H., Musters, J. J., Ratulowski, J. 1987. The apparent viscosity of foams in homogeneous beadpacks. Submitted for publication

Flumerfelt, R. W. 1980. Effects of dynamic interfacial properties on drop deformation and orientation in shear and extensional flow fields. *J. Colloid Interface Sci.* 76: 330-49

Frankel, N. A., Acrivos, A. 1970. The constitutive equation for a dilute emulsion. *J. Fluid Mech.* 44: 65–78

Gauglitz, P. A. 1986. *Instability of liquid films in constricted capillaries: a pore level description of foam generation in porous media.* PhD thesis. Univ. Calif., Berkeley. 430 pp.

Glazier, J. A., Gross, S. P., Stavans, J. 1987. Dynamics of two dimensional soap froths. *Phys. Rev. A* 36: 306–12

Hatschek, E. 1911. Die viskosität der dispersoide. *Kolloid-Z.* 8: 34–39

Hatschek, E. 1913. The general theory of viscosity of two-phase systems. *Trans. Faraday Soc.* 9: 80–92

Heller, J. P., Kuntamukkula, M. S. 1987. Critical review of the foam rheology literature. *Ind. Eng. Chem. Res.* 26: 318–25

Hirasaki, G. J., Lawson, J. B. 1985. Mechanisms of foam flow in porous media: apparent viscosity in smooth capillaries. *Soc. Pet. Eng. J.* 25: 176–90

Kelvin, Lord (Thompson, W.) 1887. On the division of space with minimum partitional area. *Philos. Mag.* 24: 503–14

Khan, S. A. 1985. *Rheology of large gas fraction liquid foams.* PhD thesis. Mass. Inst. Technol., Cambridge. 258 pp.

Khan, S. A. 1987. Foam rheology: relation between elongation and shear deformations in high gas fraction foams. *Rheol. Acta* 26: 78–84

Khan, S. A., Armstrong, R. C. 1986. Rheology of foams: I. Theory for dry foams. *J. Non-Newtonian Fluid Mech.* 22: 1–22

Khan, S. A., Armstrong, R. C. 1987. Rheology of foams: II. Effects of polydispersity and liquid viscosity for foams having gas fraction approaching unity. *J. Non-Newtonian Fluid Mech.* 25: 61–92

Kraynik, A. M. 1981. Rheological aspects of thermoplastic foam extrusion. *Polym. Eng. Sci.* 21: 80–85

Kraynik, A. M. 1982. *Aqueous foam rheology.* Presented at Ann. Meet. Soc. Rheol., Evanston, Ill.

Kraynik, A. M. 1986. *Extensional motions of spatially periodic lattices: suspension and foam rheology.* Presented at Ann. Meet. AIChE, Miami Beach, Fla.

Kraynik, A. M. 1987. Foam rheology: the

linear viscoelastic response of a spatially periodic model. *Proc. Can. Congr. Appl. Mech., 11th, Edmonton*, 2: B2–3

Kraynik, A. M., Hansen, M. G. 1986. Foam and emulsion rheology: a quasistatic model for large deformations of spatially periodic cells. *J. Rheol.* 30: 409–39

Kraynik, A. M., Hansen, M. G. 1987. Foam rheology: a model of viscous phenomena. *J. Rheol.* 31: 175–205

Landau, L., Levich, B. 1942. Dragging of a liquid by a moving plate. *Acta Physicochim. URSS* 17: 42–54

Levich, V. G. 1962. *Physicochemical Hydrodynamics*. Englewood Cliffs, NJ: Prentice-Hall. 700 pp.

Lucassen, J. 1981. Dynamic properties of free liquid films and foams. In *Anionic Surfactants—Physical Chemistry of Surfactant Action*, ed. E. H. Lucassen-Reynders, pp. 217–65. New York: Marcel Dekker. 412 pp.

Lucassen-Reynders, E. H. 1981. Surface elasticity and viscosity in compression/dilation. In *Anionic Surfactants—Physical Chemistry of Surfactant Action*, ed. E. H. Lucassen-Reynders, pp. 173–216. New York: Marcel Dekker. 412 pp.

Lyklema, J., Scholten, P. C., Mysels, K. J. 1965. Flow in thin liquid films. *J. Phys. Chem.* 69: 116–23

Mahalingam, R., Surati, H. S., Brink, J. A. 1975. High-expansion foam flow analyses. In *Advances in Interfacial Phenomena of Particulate/Solution/Gas Systems: Applications to Flotation Research*, ed. P. Somasundaran, R. B. Grieves, 71: 52–58. New York: AIChE. 191 pp.

Mannheimer, R. J. 1972. Anomalous rheological characteristics of a high-internal-phase-ratio emulsion. *J. Colloid Interface Sci.* 40: 370–82

Matalon, R. 1953. Foams. In *Flow Properties of Disperse Systems*, ed. J. J. Hermans, pp. 323–43. New York: Interscience. 445 pp.

Matzke, E. B. 1946. The three-dimensional shape of bubbles in foam—an analysis of the role of surface forces in three-dimensional cell shape determination. *Am. J. Bot.* 33: 58–80

Mooney, M. 1931. Explicit formulas for slip and fluidity. *J. Rheol.* 2: 210–22

Mysels, K. J., Cox, M. C. 1962. An experimental test of Frankel's law of film thickness. *J. Colloid Interface Sci.* 17: 136–45

Mysels, K. J., Shinoda, K., Frankel, S. 1959. *Soap Films: Studies of Their Thinning*. New York: Pergamon. 116 pp.

Pacetti, S. D. 1985. *Structural modeling of foam rheology*. MS thesis. Univ. Houston, Tex. 156 pp.

Park, C.-W., Homsy, G. M. 1984. Two-phase displacement in Hele Shaw cells: theory. *J. Fluid Mech.* 139: 291–308

Plateau, J. 1873. *Statique Expérimentale et Théorique des Liquides Soumis aux Seules Forces Moléculaires*. Paris: Gauthier-Villars. 495 pp.

Prieditis, J. 1987. *Mechanistic studies of foam displacement in porous media*. PhD thesis. Univ. Houston, Tex. In preparation

Princen, H. M. 1979. Highly concentrated emulsions. I. Cylindrical systems. *J. Colloid Interface Sci.* 71: 55–66

Princen, H. M. 1983. Rheology of foams and highly concentrated emulsions. I. Elastic properties and yield stress of a cylindrical model system. *J. Colloid Interface Sci.* 91: 160–75

Princen, H. M. 1985. Rheology of foams and highly concentrated emulsions. II. Experimental study of the yield stress and wall effects for concentrated oil-in-water emulsions. *J. Colloid Interface Sci.* 105: 150–71

Princen, H. M., Aronson, M. P., Moser, J. C. 1980. Highly concentrated emulsions. II. Real systems. *J. Colloid Interface Sci.* 75: 246–70

Princen, H. M., Kiss, A. D. 1986. Rheology of foams and highly concentrated emulsions. III. Static shear modulus. *J. Colloid Interface Sci.* 112: 427–37

Prud'homme, R. K. 1981. *Foam flow*. Presented at Ann. Meet. Soc. Rheol., Louisville, Ky.

Prud'homme, R. K., Bird, R. B. 1978. The dilatational properties of suspensions of gas bubbles in incompressible Newtonian and non-Newtonian fluids. *J. Non-Newtonian Fluid Mech.* 3: 261–79

Ransohoff, T. C. 1986. *Foam generation in constricted noncircular capillaries and in bead packs*. MS thesis. Univ. Calif., Berkeley. 207 pp.

Rosen, M. J. 1978. *Surfactants and Interfacial Phenomena*. New York: Wiley. 304 pp.

Ruschak, K. J. 1985. Coating flows. *Ann. Rev. Fluid Mech.* 17: 65–89

Schowalter, W. R., Chaffey, C. E., Brenner, H. 1968. Rheological equation of a dilute emulsion. *J. Colloid Interface Sci.* 26: 152–60

Schowalter, W. R. 1978. *Mechanics of Non-Newtonian Fluids*. Oxford: Pergamon. 300 pp.

Schwartz, L. W., Princen, H. M. 1987. A theory of extensional viscosity for flowing foams and concentrated emulsions. *J. Colloid Interface Sci.* 118: 201–11

Schwartz, L. W., Princen, H. M., Kiss, A. D. 1986. On the motion of bubbles in capillary tubes. *J. Fluid Mech.* 172: 259–75

Sibree, J. O. 1934. The viscosity of froth. *Trans. Faraday Soc.* 30: 325–31

Siehr, A. 1938. Zur Kenntnis der mechanischen Eigenschatfen von Schäumen, III. *Kolloid-Z.* 85: 70–74

Slattery, J. C., Flumerfelt, R. W. 1982. Interfacial phenomena. In *Handbook of Multiphase Systems*, ed. G. Hetsroni, pp. 1—224–73. Washington, DC: Hemisphere

Stamenovic, D., Wilson, T. A. 1984. The shear modulus of liquid foam. *J. Appl. Mech.* 51: 229–31

Tanner, R. I. 1985. *Engineering Rheology*. Oxford: Clarendon. 451 pp.

Taylor, G. I. 1932. The viscosity of a fluid containing small drops of another fluid. *Proc. R. Soc. London Ser. A* 138: 41–48

Taylor, G. I. 1954. The two coefficients of viscosity for an incompressible fluid containing air bubbles. *Proc. R. Soc. London Ser. A* 226: 34–39

Teletzke, G. F. 1983. *Thin liquid films: molecular theory and hydrodynamic implications.* PhD thesis. Univ. Minn., Minneapolis. 354 pp.

Teletzke, G. F., Davis, H. T., Scriven, L. E. 1987a. How liquids spread on solids. *Chem. Eng. Commun.* 55: 41–58

Teletzke, G. F., Davis, H. T., Scriven, L. E. 1987b. Wetting hydrodynamics. *Rev. Phys. Appl.* In press

Thondavadl, N. N., Lemlich, R. 1985. Flow properties of foam with and without solid particles. *Ind. Eng. Chem. Process Des. Dev.* 24: 748–53

Tilton, J. N. 1985. *Viscocapillary slip flows with special application to microdisplacement in porous media.* PhD thesis. Univ. Houston, Tex. 285 pp.

Walters, K. 1975. *Rheometry*. London: Chapman & Hall. 278 pp.

Weaire, D., Fu, T.-L. 1988. The mechanical behavior of foams and emulsions. *J. Rheol.* In press

Weaire, D., Kermode, J. P. 1983. Computer simulation of a two-dimensional soap froth. I. Method and motivation. *Philos. Mag. B* 48: 245–59

Weaire, D., Kermode, J. P. 1984. Computer simulation of a two-dimensional soap froth. II. Analysis of results. *Philos. Mag. B* 50: 379–95

Weaire, D., Rivier, N. 1984. Soap, cells and statistics—random patterns in two dimensions. *Contemp. Phys.* 25: 59–99

Weaire, D., Fu, T.-L., Kermode, J. P. 1986. On the shear elastic constant of a two-dimensional froth. *Philos. Mag. B* 54: L39–43

Wenzel, H. G., Brungraber, R. J., Stelson, T. E. 1970. The viscosity of high expansion foam. *J. Mater.* 5: 396–412

Wenzel, H. G., Stelson, T. E., Brungraber, R. J. 1967. Flow of high expansion foam in pipes. *Proc. Am. Soc. Civ. Eng.* EM6: 153–65

Yoshimura, A., Prud'homme, R. K., Princen, H. M., Kiss, A. D. 1987. A comparison of techniques for measuring yield stresses. *J. Rheol.* In press